NEUTRON STAR MERGER

Illuminating gravitational waves: A concordant picture of photons from a neutron star merger

M. M. Kasliwal,[1]* E. Nakar,[2] L. P. Singer,[3,4] D. L. Kaplan,[5] D. O. Cook,[1] A. Van Sistine,[5] R. M. Lau,[1] C. Fremling,[1] O. Gottlieb,[2] J. E. Jencson,[1] S. M. Adams,[1] U. Feindt,[6] K. Hotokezaka,[7,8] S. Ghosh,[5] D. A. Perley,[9] P.-C. Yu,[10] T. Piran,[11] J. R. Allison,[12,13] G. C. Anupama,[14] A. Balasubramanian,[15] K. W Bannister,[16] J. Bally,[17] J. Barnes,[18] S. Barway,[19] E. Bellm,[20] V. Bhalerao,[21] D. Bhattacharya,[22] N. Blagorodnova,[1] J. S. Bloom,[23,24] P. R. Brady,[5] C. Cannella,[1] D. Chatterjee,[5] S. B. Cenko,[3,4] B. E. Cobb,[25] C. Copperwheat,[9] A. Corsi,[26] K. De,[1] D. Dobie,[12,27,16] S. W. K. Emery,[28] P. A. Evans,[29] O. D. Fox,[30] D. A. Frail,[31] C. Frohmaier,[32,33] A. Goobar,[6] G. Hallinan,[1] F. Harrison,[1] G. Helou,[34] T. Hinderer,[35] A. Y. Q. Ho,[1] A. Horesh,[11] W.-H. Ip,[8] R. Itoh,[36] D. Kasen,[23,37] H. Kim,[38] N. P. M. Kuin,[28] T. Kupfer,[1] C. Lynch,[12,27] K. Madsen,[1] P. A. Mazzali,[9,39] A. A. Miller,[40,41] K. Mooley,[42] T. Murphy,[12,27] C.-C. Ngeow,[10] D. Nichols,[35] S. Nissanke,[35] P. Nugent,[23,24] E. O. Ofek,[43] H. Qi,[5] R. M. Quimby,[44,45] S. Rosswog,[46] F. Rusu,[47] E. M. Sadler,[12,27] P. Schmidt,[35] J. Sollerman,[46] I. Steele,[9] A. R. Williamson,[35] Y. Xu,[1] L. Yan,[1,34] Y. Yatsu,[36] C. Zhang,[5] W. Zhao[47]

Merging neutron stars offer an excellent laboratory for simultaneously studying strong-field gravity and matter in extreme environments. We establish the physical association of an electromagnetic counterpart (EM170817) with gravitational waves (GW170817) detected from merging neutron stars. By synthesizing a panchromatic data set, we demonstrate that merging neutron stars are a long-sought production site forging heavy elements by r-process nucleosynthesis. The weak gamma rays seen in EM170817 are dissimilar to classical short gamma-ray bursts with ultrarelativistic jets. Instead, we suggest that breakout of a wide-angle, mildly relativistic cocoon engulfing the jet explains the low-luminosity gamma rays, the high-luminosity ultraviolet-optical-infrared, and the delayed radio and x-ray emission. We posit that all neutron star mergers may lead to a wide-angle cocoon breakout, sometimes accompanied by a successful jet and sometimes by a choked jet.

On 17 August 2017 at 12:41:04 UTC, gravitational waves from the merger of two neutron stars (NS-NS merger) were detected by the Laser Interferometer Gravitational-Wave Observatory (LIGO) and dubbed GW170817 (*1*). Two seconds later, the first temporally coincident photons were detected as gamma rays by the Fermi satellite (*2*–*4*). GW170817 was a sufficiently loud event that the joint on-sky localization from the LIGO and Virgo interferometers was 31 square degrees (Fig. 1), with an initial distance estimate of 40 ± 8 Mpc (*5*). To identify potential host galaxies (*6*, *7*), we cross-matched the localization to our Census of the Local Universe (*8*) galaxy catalog and found only 49 galaxies in this volume (*9*, *10*). To prioritize follow-up, we ranked the galaxies by stellar mass [table S1 and the supplementary materials (*10*)]. A multitude of telescopes promptly began multiwavelength searches for an electromagnetic counterpart in and around these galaxies. Ground-based searches were systematically delayed (owing to the southern location) by half a day until sunset in Chile (*11*, *12*). A bright optical transient was identified and announced by the Swope telescope team at Las Campanas Observatory (*13*, *14*) in the third-ranked galaxy in our list, named NGC 4993. This source, SSS 17a, is located at right ascension $13^{h}09^{m}48.071^{s}$ and declination $-23^{d}22^{m}53.37^{s}$ [J2000 equinox (*10*)], with a projected offset from the nucleus of NGC 4993 of 2.2 kpc and away from any sites of star formation [fig. S1 (*10*)]. We also detected this transient in the infrared and ultraviolet wavelengths [companion paper (*15*)]. Nine days later, an x-ray counterpart was identified (*16*, *17*). Fifteen days later, a radio counterpart was identified [companion paper (*18*)].

Initially, the bright luminosity and the blue, featureless optical spectrum of SSS17a appeared to be consistent with a young supernova explosion that should brighten (figs. S2 and S3). However, on the second night, the source faded substantially in the optical and brightened in the infrared. Combining ultraviolet-optical-infrared (UVOIR) data from 24 telescopes on seven continents, we constructed a bolometric light curve [Fig. 2; details are given in (*10*)]. The bolometric luminosity evolves from 10^{42} erg s^{-1} at 0.5 days to 3×10^{40} erg s^{-1} at 10 days (Fig. 2). By estimating the blackbody effective temperature evolution, we find that the source rapidly cools from ≈11000 to ≈5000 K in a day and to ≈1400 K in 10 days. The inferred photospheric expansion velocities span 0.3*c* to 0.1*c*, where *c* is the speed of light (*10*). Furthermore, infrared spectroscopy shows broad features that do not resemble any transient seen before (Fig. 3 and figs. S4 and S5). The combination of high velocities, fast optical decline, slow infrared evolution, and broad peaks in the infrared spectra are unlike any previously known transient and unlikely to be due to a chance coincidence of an unrelated source. We thus establish that the panchromatic photons, hereafter EM170817, are spatially, temporally, and physically associated with GW170817. With this firm connection, we turn our attention to understanding the astrophysical origin of EM170817.

Evidence for nucleosynthesis of heavy elements

It is well established that chemical elements up to iron in the periodic table were produced either in the Big Bang, cores of stars, or supernova explosions. However, the origin of half the elements heavier than iron, including gold, platinum, and uranium, has remained a mystery. These heavy elements are synthesized by the rapid capture of neutrons (r-process nucleosynthesis). Some models have proposed that the decompression of neutron-rich matter in a NS-NS merger may provide suitable conditions to robustly synthesize heavy r-process elements (*19*, *20*). Radioactive decay of freshly synthesized unstable isotopes should drive transient electromagnetic emission known as a kilonova or macronova [e.g., (*21*, *22*)]. We test this hypothesis with the optical and infrared data of EM170817.

First, we compare the spectra of EM170817 with a library of astronomical transients (*10*) and theoretical models for macronova spectra (*23*). The optical spectra exhibit a featureless continuum (figs. S2 and S3). Infrared spectra (Fig. 3) have two distinct, broad peaks in the *J* band (10620 ± 1900 Å) and *H* band (15500 ± 1430 Å). Owing to the high velocities in the ejecta material, each peak may be produced by a complex blend of elements instead of a single element. Although the *J*-band peak is reminiscent of either helium or hydrogen, the corresponding feature in the *H* band seen in core-collapse supernovae is not present (fig. S5). If instead we compare with type Ia supernovae, the *J*-band peak could be similar to that of iron-group elements. However, again, the second *H*-band peak is dissimilar to that seen in type Ia supernovae (fig. S4). By comparing predictions of spectra of macronovae (*23*), based on the assumption that neodymium (Nd) is representative of lanthanides synthesized through the r-process, we find a reasonable match to both the *J*-band and *H*-band features for an ejecta mass (M_{ej}) of 0.05 solar masses ($M_{\odot}$) and velocity (v) of 0.1*c* (Fig. 3). Recent updates to these models, incorporating line transitions from 14 elements and tuning the relative abundance ratios, indicate that Nd plays a crucial role in explaining these features (*24*). We conclude that a blend of elements substantially heavier than those produced in supernovae is a viable explanation for the spectra of EM170817.

Next, we compare our infrared light curves of EM170817 (Fig. 4) with a suite of existing macronova models by various groups (*25*–*28*). The slow, red photometric evolution seen in EM170817 is a generic feature of all macronova models, despite their differing treatments of matter dynamics, matter geometry, nuclear heating, opacities, and radiation transfer. The observed late-time emission (>3 days) is fully consistent with radioactive decay of the dynamical ejecta containing elements from all three r-process abundance peaks (fig. S10). The observed luminosity, temperature, and temporal evolution roughly match model predictions for an ejecta mass of ~0.05 $M_\odot$, an ejecta velocity of ~0.1c, and an opacity (κ) of ~10 cm^2 g^{-1}.

We examine this match further with simple analytics. Dividing the observed bolometric luminosity (≈6×10^{41} erg s^{-1} at 1 day) by the β-decay heating rate of r-process elements [≈1.5×10^{10} erg s^{-1} g^{-1} (*29*)] gives a lower limit on the r-process ejecta mass of >0.02 $M_\odot$. The decline rate of the bolometric luminosity also matches that expected from the β-decay heating rate of r-process elements with the time-dependent thermalization efficiency of the decay products (Fig. 2). The expansion velocity of the ejecta (0.1c to 0.3c) derived from the photospheric radius is consistent with the results of merger simulations (*30*–*32*). Ejecta mass estimates based on observed emission are necessarily lower limits because a substantial amount of additional matter can be hidden at lower velocity.

Next, we focus on the early-time emission of EM170817, which is hotter, more luminous, and faster-rising than predicted by the suite of macronova models discussed above (Fig. 4). Decay of free neutrons would give an unphysically large ratio of neutron mass to the ejecta mass (*10*). Ultraviolet flashes predicted by (*33*, *34*) are on a much shorter time scale than that observed for EM170817. Instead, we propose two possible explanations. (i) If some fraction of the ejecta is boosted to mildly relativistic speeds, the relativistic expansion could shorten the observed peak time, and the Doppler effect could result in bluer, brighter emission. The jet cocoon model (discussed below) could accelerate enough material at higher latitudes. All material would have κ ≳ 1 cm^2 g^{-1} in this scenario. (ii) A disk-driven wind enriched with lighter r-process elements with κ ≈ 0.5 cm^2 g^{-1} could also

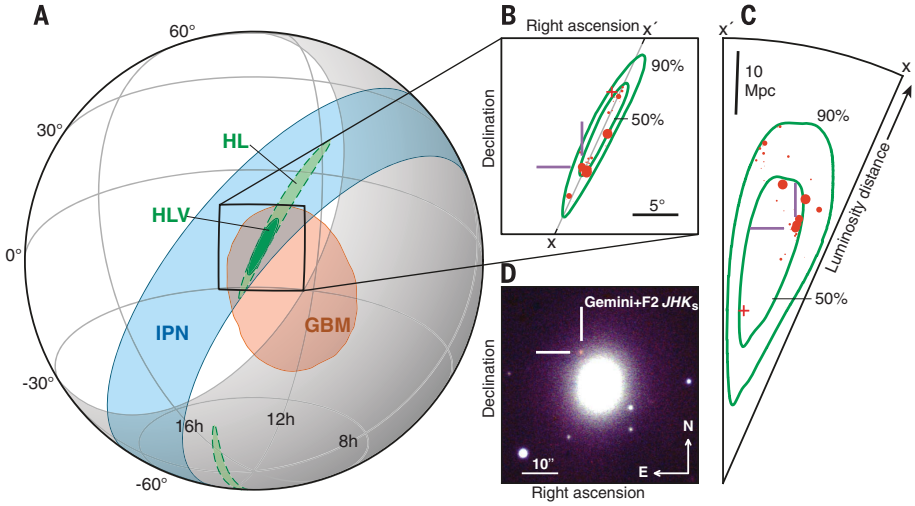

Fig. 1. Localization of GW170817 and associated transient EM170817. (**A**) Constraints at the 90% confidence level on the sky position from gravitational wave and gamma-ray observations. The rapid LIGO localization is indicated by the green dashed contour and the LIGO/Virgo localization by solid green. The Fermi Gamma-ray Burst Monitor (GRB) (*4*) is shown in orange, and the InterPlanetary Network (IPN) triangulation from Fermi and INTEGRAL is shown in blue (*50*). The shaded region is the Earth limb as seen by AstroSat, which is excluded by the nondetection by the Cadmium Zinc Telluride Imager instrument. HL, Hanford Livingston; HVL, Hanford Livingston Virgo; h, hour. (**B**) Forty-nine galaxies from the Census of the Local Universe catalog (table S3; red, with marker size proportional to the stellar mass of the galaxy) within the LIGO/Virgo three-dimensional 50% and 90% credible volumes (green). One radio-selected optically dark galaxy whose stellar mass is unknown is marked with a plus. (**C**) Cross section along the X-X′ plane from (B), showing the luminosity distances of the galaxies in comparison with the LIGO/Virgo localization. (**D**) False-color near-infrared image of EM170817 and its host galaxy NGC 4993, assembled from near-infrared observations by the FLAMINGOS-2 (F2) instrument on Gemini-South (*10*), with J, H, and K_s shown as blue, green, and red, respectively. Our K_s-band detections span 18.06 August 2017 to 5.99 September 2017, and we show 27.97 August 2017 above.

[1]Division of Physics, Math and Astronomy, California Institute of Technology, 1200 East California Boulevard, Pasadena, CA 91125, USA. [2]The Raymond and Beverly Sackler School of Physics and Astronomy, Tel Aviv University, Tel Aviv 69978, Israel. [3]Astroparticle Physics Laboratory, NASA Goddard Space Flight Center, Mail Code 661, Greenbelt, MD 20771, USA. [4]Joint Space-Science Institute, University of Maryland, College Park, MD 20742, USA. [5]Department of Physics, University of Wisconsin, Milwaukee, WI 53201, USA. [6]The Oskar Klein Centre, Department of Physics, Stockholm University, AlbaNova, SE-106 91 Stockholm, Sweden. [7]Center for Computational Astrophysics, Simons Foundation, Flatiron Institute, 162 5th Avenue, New York, NY 10010, USA. [8]Department of Astrophysical Sciences, Princeton University, Peyton Hall, Princeton, NJ 08544, USA. [9]Astrophysics Research Institute, Liverpool John Moores University, IC2, Liverpool Science Park, 146 Browlow Hill, Liverpool L3 5RF, UK. [10]Graduate Institute of Astronomy, National Central University, No. 300, Zhongda Road, Zhongli District, Taoyuan City 32001, Taiwan. [11]Racah Institute of Physics, The Hebrew University of Jerusalem, Jerusalem 91904, Israel. [12]Sydney Institute for Astronomy, School of Physics A28, The University of Sydney, New South Wales 2006, Australia. [13]Australian Research Council Centre of Excellence for All-sky Astrophysics in 3 Dimensions, Australia. [14]Indian Institute of Astrophysics, II Block Koramangala, Bangalore 560034, India. [15]Indian Institute of Science Education and Research, Dr. Homi Bhabha Road, Pashan, Pune 411008, India. [16]Australia Telescope National Facility, Astronomy and Space Science, Commonwealth Scientific and Industrial Research Organisation, Post Office Box 76, Epping, New South Wales 1710, Australia. [17]Department of Astrophysical and Planetary Sciences, University of Colorado, Boulder, CO 80305, USA. [18]Columbia Astrophysics Laboratory, Columbia University, New York, NY 10027, USA. [19]South African Astronomical Observatory, Post Office Box 9, Observatory, Cape Town 7935, South Africa. [20]Department of Astronomy, University of Washington, Seattle, WA 98195, USA. [21]Department of Physics, Indian Institute of Technology Bombay, Mumbai 400076, India. [22]Inter-University Centre for Astronomy and Astrophysics, Post Office Bag 4, Ganeshkhind, Pune 411007, India. [23]Department of Astronomy, University of California, Berkeley, CA 94720-3411, USA. [24]Lawrence Berkeley National Laboratory, 1 Cyclotron Road, MS 50B-4206, Berkeley, CA 94720, USA. [25]Department of Physics, George Washington University, Washington, DC 20052, USA. [26]Department of Physics and Astronomy, Texas Tech University, Box 41051, Lubbock, TX 79409-1051, USA. [27]Australian Research Council Centre of Excellence for All-sky Astrophysics, Australia. [28]University College London, Mullard Space Science Laboratory, Holmbury St. Mary, Dorking RH5 6NT, UK. [29]X-ray and Observational Astronomy Research Group, Leicester Institute for Space and Earth Observation, Department of Physics and Astronomy, University of Leicester, University Road, Leicester, LE1 7RH, UK. [30]Space Telescope Science Institute, 3700 San Martin Drive, Baltimore, MD 21218, USA. [31]National Radio Astronomy Observatory, Socorro, NM 87825, USA. [32]Department of Physics and Astronomy, University of Southampton, Southampton, Hampshire SO17 1BJ, UK. [33]Institute of Cosmology and Gravitation, Dennis Sciama Building, University of Portsmouth, Burnaby Road, Portsmouth PO1 3FX, UK. [34]Infrared Processing and Analysis Center, California Institute of Technology, Pasadena, CA 91125, USA. [35]Institute of Mathematics, Astrophysics and Particle Physics, Radboud University, Heyendaalseweg 135, 6525 AJ Nijmegen, Netherlands. [36]Department of Physics, Tokyo Institute of Technology, 2-12-1 Ookayama, Meguro-ku, Tokyo 152-8551, Japan. [37]Department of Physics, University of California, Berkeley, CA 94720, USA. [38]Gemini Observatory, Casilla 603, La Serena, Chile. [39]Max-Planck Institute for Astrophysics, Garching, Germany. [40]Center for Interdisciplinary Exploration and Research in Astrophysics and Department of Physics and Astronomy, Northwestern University, Evanston, IL 60208, USA. [41]The Adler Planetarium, Chicago, IL 60605, USA. [42]Astrophysics, Department of Physics, University of Oxford, Keble Road, Oxford OX1 3RH, UK. [43]Department of Particle Physics and Astrophysics, Weizmann Institute of Science, Rehovot 7610001, Israel. [44]Department of Astronomy, San Diego State University, San Diego, CA 92182, USA. [45]Kavli Institute for the Physics and Mathematics of the Universe (WPI), The University of Tokyo Institutes for Advanced Study, The University of Tokyo, Kashiwa, Chiba 277-8583, Japan. [46]The Oskar Klein Centre, Department of Astronomy, Stockholm University, AlbaNova, SE-106 91 Stockholm, Sweden. [47]School of Engineering (EECS), University of California, Merced, CA 95343, USA.
***Corresponding author. Email: mansi@astro.caltech.edu**

produce early, blue emission (*15*). This wind could be driven from a merger remnant that is a massive neutron star with an accretion torus. We could have distinguished between these two possibilities if data were available at even earlier times.

A synthesized model explaining the panchromatic photons

We discuss three models in an effort to build a self-consistent picture that explains the gamma-ray, x-ray, ultraviolet, optical, infrared, and radio photons (Fig. 5). We propose the third model because the first model is ruled out and the second model is unlikely.

A classical, on-axis short-hard gamma-ray burst: Ruled out

A classical short-hard gamma-ray burst (sGRB) is produced by a jet in the line of sight of the observer (model A in Fig. 5) that is narrow (opening angle ~ 10°) and ultrarelativistic (Lorentz factor $\Gamma \gtrsim 100$). The progenitors of sGRBs have long been hypothesized to be NS-NS mergers (*35*). However, the observed gamma-ray luminosity of EM170817 [~10^{47} erg s^{-1} (*3*, *4*)] is lower than that of typical sGRBs by four orders of magnitude (*36*, *37*). If EM170817 were simply an extremely weak sGRB, then the successful breakout of a narrow, ultrarelativistic jet would require $<3 \times 10^{-6}\ M_{\odot}$ of material that was previously ejected in the direction of the jet (*10*). If the jet opening angle were wider, it would require even less material to successfully break out (*10*). Such a low ejecta mass is contradicted by the observed bright UVOIR counterpart, which indicates $\approx 0.05\ M_{\odot}$ of ejecta. Furthermore, this scenario cannot account for the delayed onset of x-ray emission (*15*) and radio emission (*18*).

A classical, off-axis short-hard gamma-ray burst: Unlikely

Next, we consider the possibility of a classical off-axis sGRB where the observer is not in the line of sight of a strong, ultrarelativistic jet (model B in Fig. 5). Given the sharp drop in observed gamma-ray luminosity with observing angle, we find that the observer could only be off-axis by <8° (*10*). Such a slightly off-axis orientation is unlikely because only a small fraction (≈5%) of observing angles are consistent with the observational constraints. Moreover, in this scenario, EM170817 is expected to exhibit a bright afterglow at all wavelengths roughly 1 day after the NS-NS merger, when the external shock decelerates to $\Gamma \sim 10$. Initial nondetections in the radio (*18*) and x-ray (*15*) observations at this phase constrain the circum-merger environment to an implausibly low density (<10^{-6} cm^{-3}). Another problem is that a hypothetical on-axis observer of such a sGRB would expect to see photons harder than we have thus far seen in sGRBs (*10*). Thus, it is unlikely that the gamma rays were produced by a slightly off-axis sGRB.

We conclude that EM170817 is not similar to the classical population of previously observed sGRBs. Although the observed gamma rays are indicative of a relativistic outflow (with or without a jet), they must originate from a different physical mechanism (*10*). We explore the possibility of a structured jet in sGRBs with a distribution of Lorentz factors and identify multiple challenges with this model (*10*). Therefore, we next propose a model with a wide-angle mildly relativistic outflow that propagates in the observer's direction with a relatively small Lorentz factor.

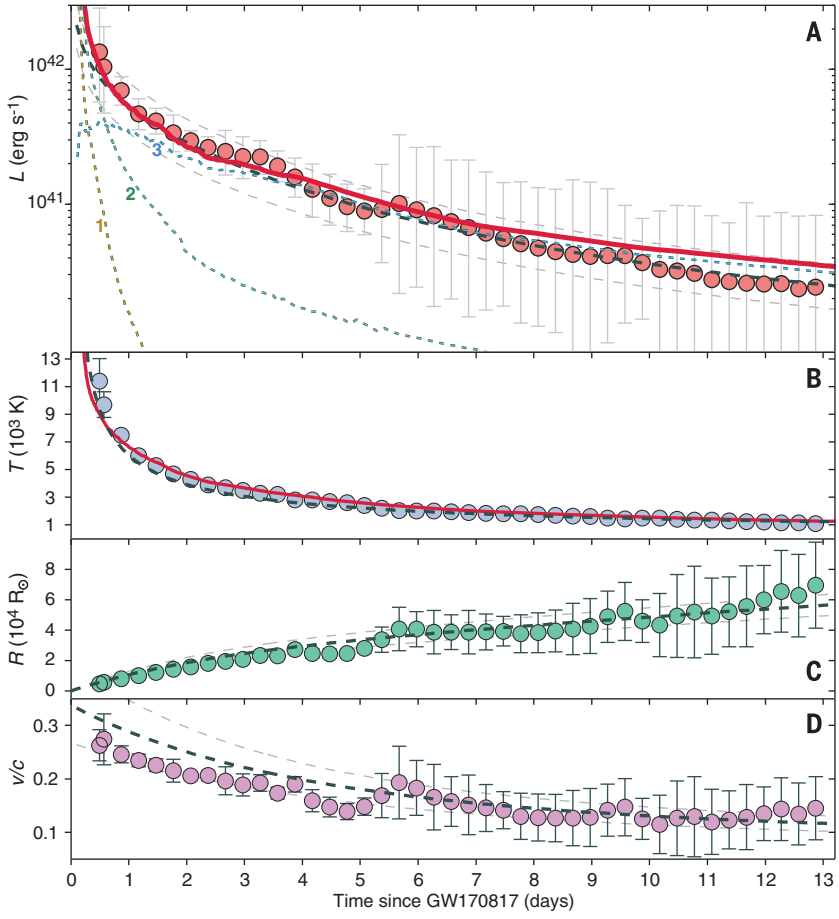

Fig. 2. The evolution of EM170817 derived from the observed spectral energy distribution. (**A**) Bolometric luminosity (*L*). (**B**) Blackbody temperature (*T*). (**C**) Photospheric radius (*R*; $R_{\odot}$, solar radius). (**D**) Inferred expansion velocity. Individual points represent blackbody fits performed at discrete epochs to which the observed photometry has been interpolated using low-order polynomial fits. Error bar details are given in (*10*). Dashed lines represent an independent Markov-Chain Monte Carlo fit without directly interpolating between data points [see (*10*) for methodology and best-fit parameter values]. The solid red lines in (A) and (B) represent the results of a hydrodynamical simulation of the cocoon model where the UVOIR emission is composed of [in (A)] cocoon cooling (yellow dashed line labeled 1), fast macronova (>0.4*c*; green dashed line labeled 2), and slow macronova (<0.4*c*; blue dashed line labeled 3).

Cocoon breakout: A concordant picture

On the basis of our UVOIR observations, we estimate that a few hundredths of a solar mass of ejecta are propelled into the circum-merger medium of a NS-NS merger with velocities spanning a few tenths the speed of light. We consider a model where a relativistic jet is launched after a short delay, perhaps because of a delayed collapse of the hypermassive neutron star into a black hole. As the jet drills through the ejecta, the material enveloping the jet inflates to form a pressurized cocoon that expands outward at mildly relativistic speeds. There are two possibilities: If the jet is wide-angle (≈30°), it will become choked and fail to drill out (model C in Fig. 5). If the jet is narrow (≈10°) and long-lived, it could penetrate the ejecta and look like a classical sGRB to an on-axis observer (model D in Fig. 5).

Independently of the fate of the jet that created the cocoon, recent numerical simulations (*34*) show that the cocoon would expand at mildly relativistic velocities ($\Gamma \approx 2$ to 3) over a wide opening angle (≈40°) with energy comparable to the jet. The cocoon has a wide enough angle and sufficient kinetic energy to easily explain the observed gamma rays. However, it remains unclear how a cocoon would dissipate its energy internally at the radius where gamma rays are observed, given its ballistic and homologous expansion

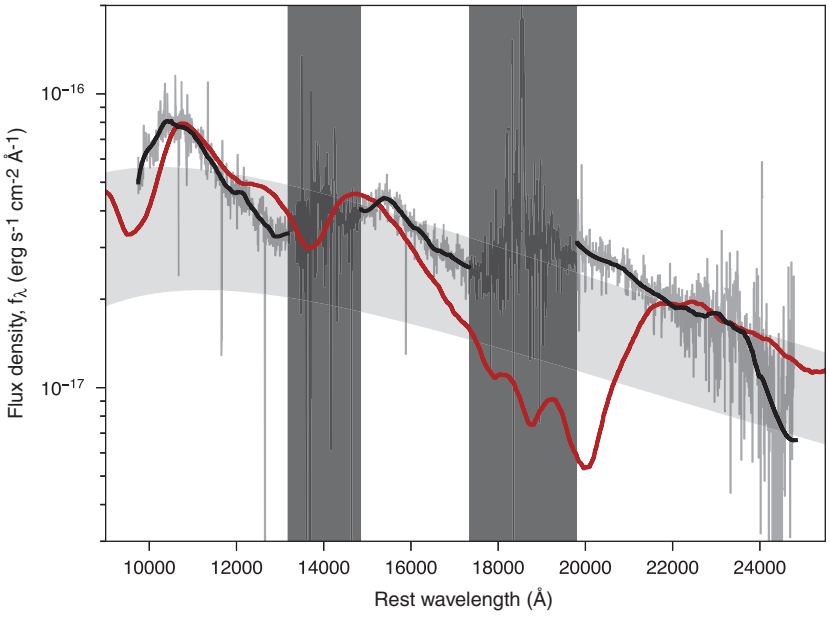

Fig. 3. Near-infrared spectrum of EM170817 at 4.5 days after merger. For display purposes, the data have been smoothed using a Savitzky-Golay filter (black line), and the unfiltered data are shown in gray. A predicted model macronova spectrum (*23*) assuming an ejecta mass of M_{ej} = 0.05 $M_\odot$ and a velocity of v = 0.1c at a phase of 4.5 days post-merger is shown in red. The spectra have been corrected for Milky Way extinction assuming reddening $E(B - V)$ = 0.1 (*10*). Regions of low signal-to-noise ratio from strong telluric absorption by Earth's atmosphere between the near-infrared *J*, *H*, and *K* spectral windows are indicated by the vertical dark gray bars. The light gray shaded band is the blackbody that best fits the photometric measurements at 4.5 days (*10*).

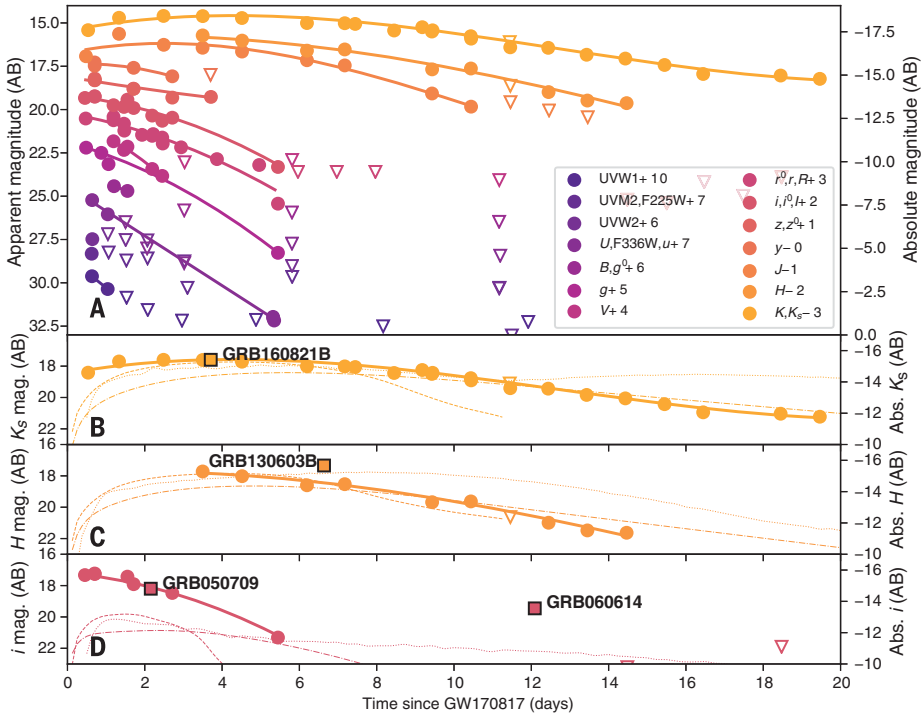

Fig. 4. Light curves of EM170817. (**A**) Multiwavelength light curve based on the ultraviolet–optical–near-infrared photometry of EM170817 [table S1 and (*10*)], plotted as AB magnitude versus time since merger and colored by wavelength. Open triangles indicate 5σ upper limits. (**B** to **D**) K_s-, *H*-, and *i*-band light curves of EM170817 with published macronova model light curves, which match well in the infrared but fail to produce the observed blue emission. For all light curves, we plot both apparent magnitude (left axis) and absolute magnitude (right axis) assuming a distance of 40 Mpc. Detections are shown as circles and upper limits as triangles. The models have been scaled to a distance of 40 Mpc and reddened with $E(B - V)$ = 0.1 (*10*). The model light curve parameters are as follows: M_{ej} = 0.05 $M_\odot$, v_{ej} = 0.1c from (*51*), model N4 with the DZ31 mass formula from (*27*), and γA2 at a viewing angle of 30° from (*28*). Optical and near-infrared observations of previously observed short gamma-ray bursts that appeared abnormally bright are shown as squares (scaled to 40 Mpc and corrected for time dilation). GRB 080503 (*52*) would have had to be at a redshift of 0.22 to be consistent. GRB 060614 (*53*) is too luminous at late times. The excess emissions observed in GRB 160821B (*40*), GRB 130603B (*39*), and GRB 050709 (*41*) appear to be similar to that observed in EM170817.

(unlike sGRB jets, which are expected to be variable with irregular internal velocities and a structure that can dissipate the jet energy by internal shocks or magnetic reconnection). A wide-angle mildly relativistic cocoon, reported in (*34*), was recently proposed as a source of wide-angle gamma-ray emission (*38*). However, this was based on an ad hoc dissipation process that is somehow at work near the photosphere (*38*). We suggest that the dissipation mechanism is the interaction of the cocoon with the ejecta and that the observed gamma rays result from the breakout of the mildly relativistic shock (driven by the cocoon) from the leading edge of the ejecta. We find that such a breakout can explain all properties of the observed low-luminosity gamma rays if its Lorentz factor is ≈2 to 3 and the breakout radius is ~3 × 10^{11} cm (*10*).

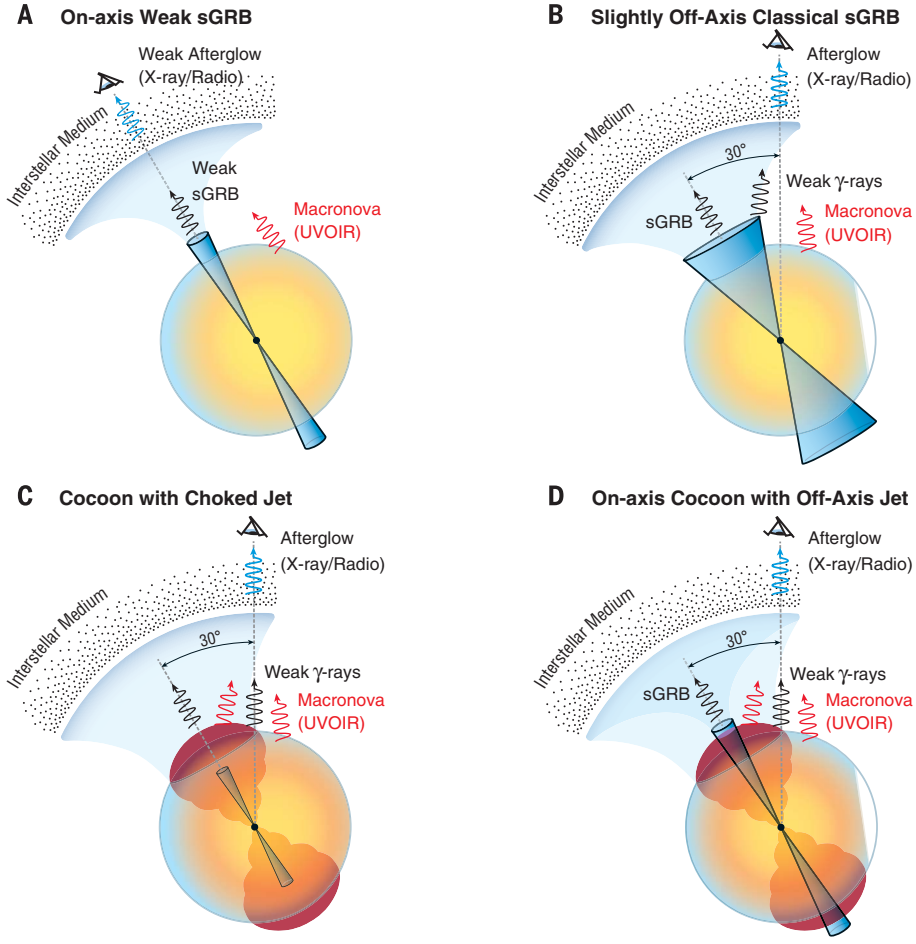

Fig. 5. Model schematics considered in this paper. In each panel, the eye indicates the line of sight to the observer. (**A**) A classical, on-axis, ultrarelativistic, weak short-hard gamma-ray burst (sGRB). (**B**) A classical, slightly off-axis, ultrarelativistic, strong sGRB. (**C**) A wide-angle, mildly relativistic, strong cocoon with a choked jet. (**D**) A wide-angle, mildly relativistic, weak cocoon with a successful off-axis jet.

We performed a relativistic hydrodynamical simulation in which a jet is injected into expanding ejecta to verify this model for EM170817 (*10*). We find that even if a minute amount of ejecta ($\approx 3 \times 10^{-9}\ M_{\odot}$) moves at $0.8c$, the breakout radius and velocity match those needed to produce the observed gamma rays for a wide range of ejecta and jet properties (*10*). For example, in the simulation shown in Fig. 6, a shock with $\Gamma \approx 2.5$ breaks out 10 s after the merger at a radius of 2.4×10^{11} cm, generating gamma-ray emission that would be observed with a delay of 2 s with respect to merger time [consistent with the Fermi observations (*3*, *4*)]. After the cocoon breaks out, the photons that were deposited by the shock diffuse outward and produce a cooling emission that fades on time scales of hours (*34*). After a few hours, radioactive decay of r-process elements becomes the dominant source of the observed emission. The emission during the first day is dominated by fast cocoon material ($v \approx 0.4c$), which is composed of high-latitude, low-opacity ($\kappa \sim 1\ \mathrm{cm^2\ g^{-1}}$) ejecta that was accelerated by the jet to high velocities. After a few days, the slower, higher-opacity ($\kappa \sim 10\ \mathrm{cm^2\ g^{-1}}$) dynamical ejecta begins to dominate the emission. We find that the bolometric light curve evolution and the temperature evolution predicted by this simulation is consistent with our UVOIR observations (Fig. 2).

The available radio and x-ray data are broadly consistent with both cocoon scenarios, albeit with slightly different circum-merger densities (*15*, *18*). If the jet is choked, the radio and x-ray data could be explained by the forward shock that the expanding cocoon drives into the circum-merger medium. If the jet is successful, the radio and x-ray data could be explained as a widely off-axis afterglow of the jet. If this emission is from the forward shock of a cocoon, we predict that the x-rays and radio will continue to rise. On the other hand, if this emission is from a widely off-axis afterglow of the jet, we predict that it will evolve slowly and eventually fade. In both scenarios, a cocoon would be needed to explain the gamma rays. We conclude that the cocoon model can self-consistently explain the multiwavelength properties of EM170817 spanning gamma rays to radio.

Implications

First, we consider whether EM170817 was an exceptional event or whether multimessenger detections will soon become routine. The large ejecta masses and high velocities observed in EM170817 suggest that intrinsically luminous UVOIR macronova emission should accompany every NS-NS merger. If our proposed mildly relativistic cocoon model is correct, the wide opening angle of the cocoon implies that gamma rays would be emitted toward the observer in about 30% of NS-NS mergers. If the jet is choked, we expect to see late onset of radio and x-ray emission from the cocoon forward shock. If the jet producing the cocoon successfully breaks out, the source would appear either as a classical wide off-axis afterglow or a classical on-axis afterglow, depending on the observer's line of sight. The launch of a successful on-axis cocoon jet may already have been evident in previous reports of possible late-time excess optical or infrared emission in sGRBs attributed to macronovae. In Fig. 4, we show that the excess emissions seen in GRB 130603B (*39*), GRB 160821B (*40*), and GRB 050709 (*41*) are roughly consistent with our observed light curve for EM170817. Separately, a plateau in the distribution of durations of sGRBs may indicate that a large fraction of sGRBs have choked jets (*42*). Joint gravitational wave and electromagnetic observations of NS-NS mergers will shed light on

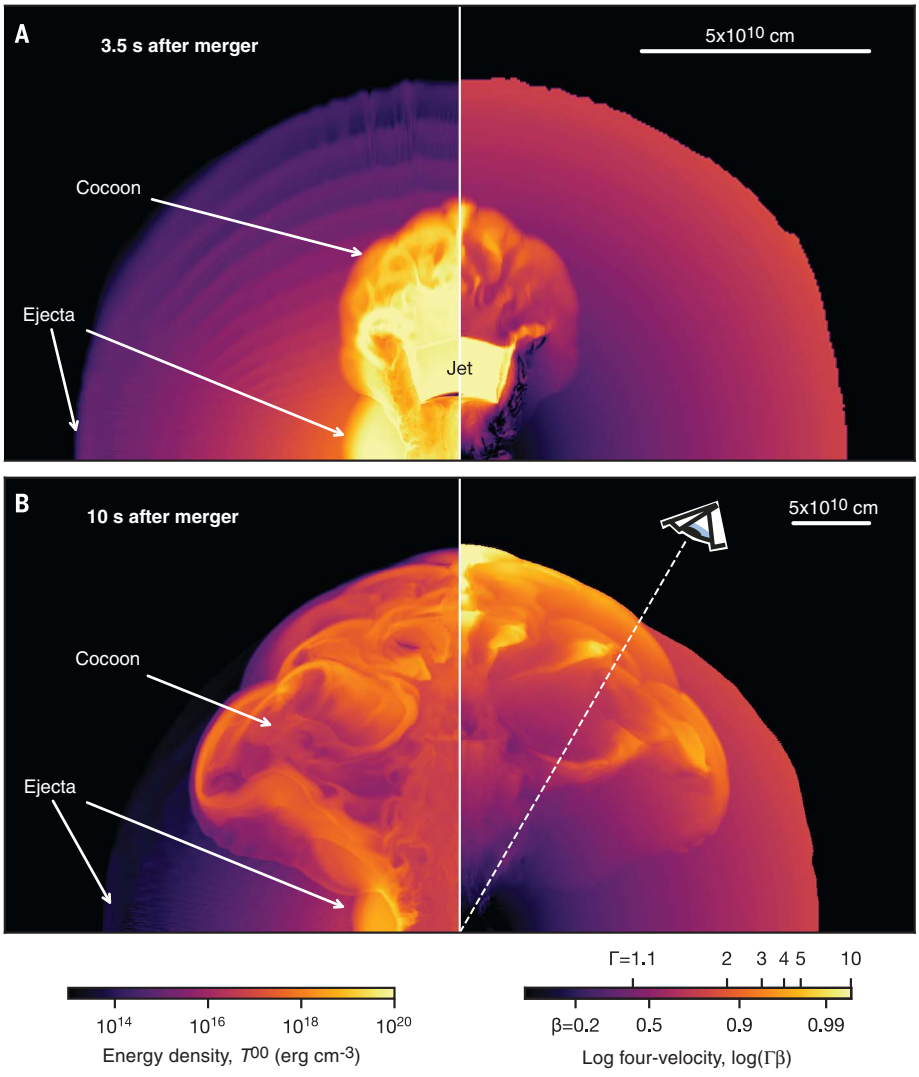

Fig. 6. Snapshots from a hydrodynamic simulation of a cocoon generated by a choked jet with emission consistent with EM170817. The left half-plane is color-coded by logarithmic energy density (ergs per cubic centimeter) and depicts the energetics. The right half-plane is color-coded by logarithmic four-velocity (Γβ) and depicts the kinematics. The observer is at an angle of 40°, the ejecta mass is 0.1 $M_{\odot}$, and the jet luminosity is 2.6 × 10^{51} erg s^{-1}. On the basis of this simulation, a bolometric light curve was calculated, shown in Fig. 2. (**A**) This snapshot is taken at 3.5 s, shortly after the jet injection stops. The jet is fully choked by 4 s. (**B**) This snapshot is taken at 10 s, when the cocoon breaks out. The breakout radius is 2.4 × 10^{11} cm, which corresponds to 8 light-seconds. Thus, the delay between the observed gamma-ray photons and the NS-NS merger is the difference between these times, 2 s. The Lorentz factor of the shock upon breakout is between 2 and 3. Details are given in (*10*).

the relative fractions of cocoons with choked and successful jets.

Next, we consider whether NS-NS mergers could be the primary sites of r-process nucleosynthesis. This depends on both the rate of NS-NS mergers and the average amount of r-process material synthesized per merger. On the basis of the macronova light curve, we estimate a lower limit on the mass of the produced r-process elements in EM170817 to be $M_{ej} \approx 0.05\ M_{\odot}$. The solar abundance pattern shows that the first of three r-process peaks accounts for ≈80% of the total r-process abundance [fig. S10 and (*10*)]. To account for the observed solar abundance in all three r-process peaks with NS-NS mergers, we would need a rate of ~500 Gpc^{-3} $year^{-1}$ $(M_{ej}/0.05\ M_{\odot})^{-1}$. To account for the observed abundance in the two heavier r-process peaks with NS-NS mergers, the rate would only need to be ~100 Gpc^{-3} $year^{-1}$. On the basis of the detection of GW170817, a NS-NS merger rate of 320 to 4740 Gpc^{-3} $year^{-1}$ was estimated at 90% confidence (*1*). This is larger than the classical sGRB beaming-corrected rate (*43*, *44*) and larger than the fraction of NS-NS mergers predicted on the basis of the galactic population (*45*). From an archival search for transients like EM170817 in the Palomar Transient Factory database, we find a 3σ upper limit on the rate of 800 Gpc^{-3} $year^{-1}$ (*10*). Therefore, the large ejecta mass of EM170817 and the high rate estimates for GW170817 and EM170817 are consistent with NS-NS mergers being the main production sites of r-process elements in the Milky Way [as predicted by (*19*)].

The high rate, the wide angle for contemporaneous gamma rays, the bright UVOIR emission, the forward shock producing a late onset of x-rays and radio, the increase in sensitivity of gravitational wave interferometers, and the increase in sensitivity of electromagnetic facilities [e.g., (*46*–*49*)]—all suggest that we will soon be able to jointly study many more events like GW170817 and EM170817.

REFERENCES AND NOTES

1. The LIGO Scientific Collaboration, The Virgo Collaboration, *Phys. Rev. Lett.* **119**, 161101 (2017).
2. A. Goldstein *et al.*, *Gamma Ray Coordinates Network Circular* 21528 (2017); available at https://gcn.gsfc.nasa.gov/other/G298048.gcn3.
3. B. P. Abbott *et al.*, *Astrophys. J.* **848**, L13 (2017).
4. A. Goldstein *et al.*, *Astrophys. J.* **848**, L14 (2017).
5. The LIGO Scientific Collaboration, The Virgo Collaboration, *Gamma Ray Coordinates Network Circular* 21513 (2017); available at https://gcn.gsfc.nasa.gov/other/G298048.gcn3.
6. N. Gehrels *et al.*, *Astrophys. J.* **820**, 136 (2016).
7. S. Nissanke, M. Kasliwal, A. Georgieva, *Astrophys. J.* **767**, 124 (2013).
8. D. Cook *et al.*, arXiv:1710.05016 [astro-ph.GA] (13 October 2017).
9. D. Cook, A. Van Sistine, L. Singer, M. Kasliwal, *Gamma Ray Coordinates Network Circular* 21519 (2017); available at https://gcn.gsfc.nasa.gov/other/G298048.gcn3.
10. See the supplementary materials.
11. M. M. Kasliwal, S. Nissanke, *Astrophys. J.* **789**, L5 (2014).
12. L. P. Singer *et al.*, *Astrophys. J.* **795**, 105 (2014).
13. D. Coulter *et al.*, *Gamma Ray Coordinates Network Circular* 21529 (2017); available at https://gcn.gsfc.nasa.gov/other/G298048.gcn3.
14. D. A. Coulter *et al.*, *Science* **358**, 1556–1558 (2017).
15. P. A. Evans *et al.*, *Science* **358**, 1565–1570 (2017).
16. E. Troja, L. Piro, T. Sakamoto, B. Cenko, A. Lien, *Gamma Ray Coordinates Network Circular* 21765 (2017); available at https://gcn.gsfc.nasa.gov/other/G298048.gcn3.
17. E. Troja *et al.*, *Nature* **551**, 71–74 (2017).
18. G. Hallinan *et al.*, *Science* **358**, 1579–1583 (2017).
19. J. M. Lattimer, D. N. Schramm, *Astrophys. J.* **192**, L145 (1974).
20. C. Freiburghaus, S. Rosswog, F. Thielemann, *Astrophys. J.* **525**, L121–L124 (1999).
21. L.-X. Li, B. Paczyński, *Astrophys. J.* **507**, L59–L62 (1998).
22. R. Fernández, B. D. Metzger, *Annu. Rev. Nucl. Part. Sci.* **66**, 23–45 (2016).
23. J. Barnes, D. Kasen, *Astrophys. J.* **775**, 18 (2013).
24. D. Kasen, B. Metzger, J. Barnes, E. Quataert, E. Ramirez-Ruiz, *Nature* **551**, 80–84 (2017).
25. D. Kasen, N. R. Badnell, J. Barnes, *Astrophys. J.* **774**, 25 (2013).
26. M. Tanaka, K. Hotokezaka, *Astrophys. J.* **775**, 113 (2013).
27. S. Rosswog *et al.*, *Class. Quantum Gravity* **34**, 104001 (2017).
28. R. T. Wollaeger *et al.*, arXiv:1705.07084 [astro-ph.HE] (19 May 2017).
29. K. Hotokezaka *et al.*, *Mon. Not. R. Astron. Soc.* **459**, 35–43 (2016).
30. K. Hotokezaka *et al.*, *Phys. Rev. D* **87**, 024001 (2013).
31. A. Bauswein, S. Goriely, H.-T. Janka, *Astrophys. J.* **773**, 78 (2013).
32. S. Rosswog, *Philos. Trans. A Math. Phys. Eng. Sci.* **371**, 20120272 (2013).
33. M. A. Aloy, H.-T. Janka, E. Müller, *Astron. Astrophys.* **436**, 273–311 (2005).
34. O. Gottlieb, E. Nakar, T. Piran, arXiv:1705.10797 [astro-ph.HE] (30 May 2017).
35. D. Eichler, M. Livio, T. Piran, D. N. Schramm, *Nature* **340**, 126–128 (1989).

36. E. Nakar, *Phys. Rep.* **442**, 166–236 (2007).
37. W. Fong, E. Berger, R. Margutti, B. A. Zauderer, *Astrophys. J.* **815**, 102 (2015).
38. D. Lazzati, D. Lopez-Camara, M. Cantiello, B. J. Morsony, R. Perna, J. C. Workman, arXiv:1709.01468 [astro-ph.HE] (5 September 2017).
39. N. R. Tanvir *et al*., *Nature* **500**, 547–549 (2013).
40. M. M. Kasliwal, O. Korobkin, R. M. Lau, R. Wollaeger, C. L. Fryer, *Astrophys. J.* **843**, L34 (2017).
41. Z.-P. Jin *et al*., *Nat. Commun.* **7**, 12898 (2016).
42. R. Moharana, T. Piran, arXiv:1705.02598 [astro-ph.HE] (7 May 2017).
43. D. Wanderman, T. Piran, *Mon. Not. R. Astron. Soc.* **448**, 3026–3037 (2015).
44. Z-P. Jin *et al*., arXiv:1708.07008 [astro-ph.HE] (23 August 2017).
45. E. S. Phinney, *Astrophys. J.* **380**, L17 (1991).
46. E. Bellm, S. Kulkarni, *New Astron.* **1**, 0071 (2017).
47. A. M. Moore *et al*., *Proc. SPIE* **9906**, 99062C (2016).
48. N. Ganot *et al*., *Astrophys. J.* **820**, 57 (2016).
49. S. B. Cenko *et al*., in *American Astronomical Society Meeting Abstracts*, vol. 229 (2017), p. 328.04.
50. D. Svinkin, *et al., Gamma Ray Coordinates Network Circular* 21515 (2017); available at https://gcn.gsfc.nasa.gov/other/G298048.gcn3.
51. J. Barnes, D. Kasen, M.-R. Wu, G. Martínez-Pinedo, *Astrophys. J.* **829**, 110 (2016).
52. D. A. Perley *et al*., *Astrophys. J.* **696**, 1871–1885 (2009).
53. B. Yang *et al*., *Nat. Commun.* **6**, 7323 (2015).

ACKNOWLEDGMENTS

We thank I. Kostadinova for seamlessly coordinating the GROWTH (Global Relay of Observatories Watching Transients Happen) project; B. Griswold for beautiful graphic art; P. Whitelock for facilitating InfraRed Survey Facility observations; S. Barthelmy for setting up a Ligo Virgo Consortium Gamma-ray Coordination Network system that facilitated quick, citable communication between astronomers and maximized the science return; S. Phinney, S. Kulkarni, and L. Bildsten for valuable comments; the staff of Gemini Observatory, particularly the director, L. Ferrarese, for rapidly approving our Director's Discretionary Time request; and our program contact scientists M. Shirmer, H. Kim, K. Silva, M. Andersen, and R. Salinas for supporting and executing observations. We are especially grateful to Gemini for postponing scheduled maintenance on the FLAMINGOS-2 instrument to allow us to obtain as much data as possible on this extraordinary event. This work was supported by the GROWTH project funded by the National Science Foundation under Partnerships for International Research and Education grant no. 1545949. GROWTH is a collaborative project among the California Institute of Technology (USA), University of Maryland College Park (USA), University of Wisconsin Milwaukee (USA), Texas Tech University (USA), San Diego State University (USA), Los Alamos National Laboratory (USA), Tokyo Institute of Technology (Japan), National Central University (Taiwan), Indian Institute of Astrophysics (India), Inter-University Center for Astronomy and Astrophysics (India), Weizmann Institute of Science (Israel), The Oskar Klein Centre at Stockholm University (Sweden), Humboldt University (Germany), and Liverpool John Moores University (UK). Full facility and funding acknowledgements are provided in the supplementary materials. The photometric data that we used are tabulated in table S1. All of our raw observations are available in observatory archives; URLs and project numbers are provided in the supplementary materials. The PLUTO software used for our simulations is available at http://plutocode.ph.unito.it/; our simulation input and output files are provided as data S1 and S2.

SUPPLEMENTARY MATERIALS

www.sciencemag.org/content/358/6370/1559/suppl/DC1
Materials and Methods
Supplementary Text
Figs. S1 to S10
Tables S1 to S3
References (*54–184*)
Movie S1
Data S1 and S2
Interactive Light Curves for SSS17a

14 September 2017; accepted 5 October 2017
Published online 16 October 2017
10.1126/science.aap9455

Science

Illuminating gravitational waves: A concordant picture of photons from a neutron star merger

M. M. Kasliwal, E. Nakar, L. P. Singer, D. L. Kaplan, D. O. Cook, A. Van Sistine, R. M. Lau, C. Fremling, O. Gottlieb, J. E. Jencson, S. M. Adams, U. Feindt, K. Hotokezaka, S. Ghosh, D. A. Perley, P.-C. Yu, T. Piran, J. R. Allison, G. C. Anupama, A. Balasubramanian, K. W. Bannister, J. Bally, J. Barnes, S. Barway, E. Bellm, V. Bhalerao, D. Bhattacharya, N. Blagorodnova, J. S. Bloom, P. R. Brady, C. Cannella, D. Chatterjee, S. B. Cenko, B. E. Cobb, C. Copperwheat, A. Corsi, K. De, D. Dobie, S. W. K. Emery, P. A. Evans, O. D. Fox, D. A. Frail, C. Frohmaier, A. Goobar, G. Hallinan, F. Harrison, G. Helou, T. Hinderer, A. Y. Q. Ho, A. Horesh, W.-H. Ip, R. Itoh, D. Kasen, H. Kim, N. P. M. Kuin, T. Kupfer, C. Lynch, K. Madsen, P. A. Mazzali, A. A. Miller, K. Mooley, T. Murphy, C.-C. Ngeow, D. Nichols, S. Nissanke, P. Nugent, E. O. Ofek, H. Qi, R. M. Quimby, S. Rosswog, F. Rusu, E. M. Sadler, P. Schmidt, J. Sollerman, I. Steele, A. R. Williamson, Y. Xu, L. Yan, Y. Yatsu, C. Zhang and W. Zhao

Science **358** (6370), 1559-1565.
DOI: 10.1126/science.aap9455originally published online October 16, 2017

GROWTH observations of GW170817

The gravitational wave event GW170817 was caused by the merger of two neutron stars (see the Introduction by Smith). In three papers, teams associated with the GROWTH (Global Relay of Observatories Watching Transients Happen) project present their observations of the event at wavelengths from x-rays to radio waves. Evans *et al.* used space telescopes to detect GW170817 in the ultraviolet and place limits on its x-ray flux, showing that the merger generated a hot explosion known as a blue kilonova. Hallinan *et al.* describe radio emissions generated as the explosion slammed into the surrounding gas within the host galaxy. Kasliwal *et al.* present additional observations in the optical and infrared and formulate a model for the event involving a cocoon of material expanding at close to the speed of light, matching the data at all observed wavelengths.

Science, this issue p. 1565, p. 1579, p. 1559; see also p. 1554

Science (print ISSN 0036-8075; online ISSN 1095-9203) is published by the American Association for the Advancement of Science, 1200 New York Avenue NW, Washington, DC 20005.